PCCP

Accepted Manuscript

ROYAL SOCIETY OF CHEMISTRY

www.rsc.org/pccp

Cite this: DOI: 10.1039/c0xx00000x

www.rsc.org/xxxxxx

ARTICLE TYPE

A Novel Strategy to Directly Fabricate Flexible Hollow Nanofibers with Tunable Luminescence-Electricity-Magnetism Trifunctionality Using One-Pot Electrospinning

Yawen Liu, Qianli Ma, Xiangting Dong*, Wensheng Yu, Jinxian Wang, Guixia Liu

Received (in XXX, XXX) Xth XXXXXXXXX 20XX, Accepted Xth XXXXXXXXX 20XX
DOI: 10.1039/b000000x

Novel photoluminescent-electrical-magnetic trifunctional flexible $Eu(BA)_3phen/PANI/Fe_3O_4/PVP$ (BA = benzoic acid, phen = phenanthroline, PANI = polyaniline, PVP = polyvinylpyrrolidone) hollow nanofibers were fabricated by one-pot electrospinning technique using specially designed coaxial spinneret for the first time. Very different from the traditional preparation process of hollow fibers via coaxial electrospinning, which need to firstly fabricate the coaxial fibers and followed by removing the core through high-temperature calcination or solvent extraction, in our current study, no core spinning solution is used to directly fabricate hollow nanofibers. The morphology and properties of the obtained hollow nanofibers were characterized in detail by X-ray diffractometry, scanning electron microscopy, transmission electron microscopy, fluorescence spectroscopy, Fourier-transform infrared spectroscopy, 4-point probes resistivity measurement system and vibrating sample magnetometry. The $Eu(BA)_3phen/PANI/Fe_3O_4/PVP$ hollow nanofibers, with outer diameters of *ca.* 305 nm and inner diameters of about 140 nm, exhibit excellent photoluminescence performance, electrical conductivity and magnetic properties. Fluorescence emission peaks of Eu^{3+} are observed in the $Eu(BA)_3phen/PANI/Fe_3O_4/PVP$ hollow nanofibers and assigned to the $^5D_0 \rightarrow {}^7F_0$ (580 nm), $^5D_0 \rightarrow {}^7F_1$ (592 nm) and $^5D_0 \rightarrow {}^7F_2$ (616 nm) energy level transitions of Eu^{3+} ions, and the $^5D_0 \rightarrow {}^7F_2$ hypersensitive transition at 616 nm is the predominant emission peak. The electrical conductivity of the hollow nanofibers reaches up to the order of 10^{-3} $S \cdot cm^{-1}$. The luminescent intensity, electrical conductivity and magnetic properties of the hollow nanofibers can be tuned by adding various amounts of $Eu(BA)_3phen$, PANI and Fe_3O_4 nanoparticles. The new-typed photoluminescent-electrical-magnetic trifunctional flexible hollow nanofibers hold potential for a variety of applications, including electromagnetic interference shielding, microwave absorption, molecular electronics and biomedicine. This design conception and synthetic strategy developed in this study are of universal significance to construct other multifunctional hollow one-dimensional nanomaterials.

1 Introduction

More recently, with the rapid development of materials science, much emphasis has been put on hollow micro/nanomaterials owing to their promising applications, such as catalysis[1], drug release[2], sensoring[3], energy storage[4] and biomedical engineering[5]. One-dimensional (1D) hollow nanomaterials, including nanotubes and hollow nanofibers, have attracted increasing interest during past decades because of their unique structure, high surface area and novel properties. Compared with common solid nanofibers, hollow nanofibers double the surface area and exhibit potential in surface-related applications such as chemical sensors[6] or photocatalysis[7, 8].

Nanocomposites are the hot spots of research in the field of functional materials. In the past few years, a great deal of work has been done to study nanocomposites with multifunctionality, which greatly expanded the application of nanocomposites in various fields.[9-11] For instance, rare earth (RE)-doped luminescent materials are usually integrated with magnetic nanoparticles (NPs) to prepare magnetic-photoluminescent bifunctional nanocomposites.[12-14] To date, except the above-mentioned zero-dimensional nanocomposites, multifunctional nanocomposites with 1D structure have been extensively pursued by scientists. Ma, et al.[15, 16] fabricated Fe_3O_4/RE complexes/polyvinylpyrrolidone (PVP) magnetic-photoluminescent bifunctional core-shell nanocables and nanobelts via electrospinning process. Wang, et al.[17] prepared Fe_2O_3/[Eu(DBM)$_3$(Bath)] (DBM = dibenzoylmethanate, Bath = bathophenanthroline)/PVP magnetic-photoluminescent bifunctional composite nanofibers. Polyaniline (PANI) is one of the most important conducting polymers due to its high conductivity, good processibility and environmental stability, as well as its potential for a variety of applications. Huang, et al.[18]

synthesized Fe_3O_4/PANI composite nanofibers via micro-emulsion polymerization of aniline in the presence of Fe_3O_4 NPs. Lv, et al.[19] fabricated [PANI/PVP]//[Eu(BA)$_3$phen/PVP] (BA = benzoic acid, phen = phenanthroline) electrical-photoluminescent bifunctional bistrand-aligned nanobundles through specially designed parallel spinnerets electrospinning technology.

Electrospinning has been proved to be an outstanding technique to process viscous solutions or melts into continuous fibers with 1D nanostructure.[20] This method not only attracts extensive academic investigations, but is also applied in many areas such as filtration[21], luminescent materials[22, 23], biological scaffolds[24], electrode materials[25] and nanocables[26]. Recent efforts have been made to improve electrospinning method and setup, and nanofibers with novel structures, such as core-sheath, Janus, porous and hollow morphology, can be prepared if appropriate processing parameters are adopted.[27-31] In many cases, nanofibers with hollow structure were prepared by coaxial electrospinning technique, in which coaxial spinnerets replace the single spinneret in the conventional setup for electrospinning, followed by appropriate post-treatment, such as core solvent extracting or calcination process. Lee, et al.[32] developed highly porous polymeric hollow nanofibers using a method based on coaxial electrospinning with inner silicon oil and outer polymer solutions, and then the silicon oil was extracted by soaking the fibers in n-hexane overnight. Li, et al.[33] successfully synthesized YF_3:Eu^{3+} hollow nanofibers via fluorination of the relevant Y_2O_3:Eu^{3+} hollow nanofibers which were obtained by calcining the coaxial electrospun core–sheath composite nanofibers. Nevertheless, the core-removing method usually affects not only the core but also the shell, and do not fit to all the situations. Therefore, it is necessary to explore more universal methods to prepare hollow structured nanofibers.

Herein, we employ one-pot electrospinning technique by using specially designed coaxial spinnerets to directly assemble photoluminescence-electricity-magnetism trifunction into flexible hollow nanofibers. We discovered a peculiar phenomenon using coaxial electrospinning apparatus that the hollow structured nanofibers can be directly obtained without using core spinning solution. Based on this method, Eu(BA)$_3$phen/PANI/Fe_3O_4/PVP hollow nanofibers have been successfully fabricated. To the best of our knowledge, up to now there is no report on the synthesis of novel hollow structured nanofibers possessing trifunctionality of photoluminescence, electricity and magnetism. More importantly, the synthetic strategy developed in this work can be extended to fabricate other hollow nanofibrous polymer-templated materials, making the strategy widely applicable for preparing advanced multifunctional materials. The hollow structure of this kind of nanofiber makes it a potential material for applications of drug targeting, bioseparation and other fields. For example, various drugs can be encapsulated into the inner of the hollow nanofibers and control the release of drug molecules, thus realizing drug target delivering and slow releasing.

2 Experimental sections

2.1 Materials

PVP K90 (Mw ≈ 130,0000), Eu_2O_3, BA, phen, $FeCl_3\cdot 6H_2O$, $FeSO_4\cdot 7H_2O$, NH_4NO_3, polyethyleneglycol (PEG, Mw ≈ 20,000), ammonia, oleic acid (OA), aniline (ANI), (IS)-(+)-camphor-10 sulfonic acid (CSA), ammonium persulfate (APS), anhydrous ethanol, $CHCl_3$, *N,N*-dimethylformamide (DMF), nitric acid and deionized water were used. All the reagents were of analytical grade and used directly as received without further purification. The purity of Eu_2O_3 was 99.99%. The deionized water was homemade.

2.2 Preparation

Synthesis of europium complexes

Eu(BA)$_3$phen powders were synthesized according to the traditional method as described in the reference[34]. 1.7596 g of Eu_2O_3 was dissolved in 10 mL of concentrated nitric acid and then crystallized by evaporation of excess nitric acid and water at the temperature of 120 °C, and $Eu(NO_3)_3\cdot 6H_2O$ was acquired. $Eu(NO_3)_3$ ethanol solution was prepared by adding 10 mL of anhydrous ethanol into the above $Eu(NO_3)_3\cdot 6H_2O$. 3.6636 g of BA and 1.9822 g of phen were dissolved in 100 mL of ethanol. The $Eu(NO_3)_3$ solution was then added into the mixture solution of BA and phen with magnetic agitation for 3 h at 60 °C. Finally, the precipitate was collected by filtration and dried at 60 °C for 12 h.

Preparation of OA modified Fe_3O_4 NPs

Fe_3O_4 NPs with the particle size of 8-10 nm were obtained via a facile coprecipitation synthetic method[35]. To improve the monodispersity, stability, and solubility of Fe_3O_4 NPs in the spinning solution, PEG was used as the protective agents to prevent the particles from aggregation, and the as-prepared Fe_3O_4 NPs were coated with OA. A typical synthetic procedure is as follows: 5.4060 g of $FeCl_3\cdot 6H_2O$, 2.7800 g of $FeSO_4\cdot 7H_2O$, 4.04 g of NH_4NO_3 and 1.9 g of PEG were added into 100 mL of deionized water to form a uniform solution under vigorous stirring at 50 °C. At the same time, the reactive mixture was kept under argon atmosphere to prevent the oxidation of Fe^{2+}. After the mixture had been bubbled with argon for 30 min, 0.1 mol·L^{-1} of $NH_3\cdot H_2O$ was dropwise added into the mixture to adjust pH value above 11. Then the system was continuously bubbled with argon for 20 min at 50 °C, and black precipitates were formed. Per 1.0000 g of the as-prepared Fe_3O_4 NPs were ultrasonically dispersed in 50 mL of deionized water for 20 min. The suspension was subsequently heated to 80 °C under argon atmosphere with vigorous mechanical stirring for 30 min and then 0.5 mL of OA was slowly added. The reaction was stopped after heating and stirring the mixture for 40 min. The precipitates were collected from the solution by magnetic separation, washed with anhydrous ethanol for three times, and then dried in an electric vacuum oven at 60 °C for 6 h. The dosages of deionized water and OA were adjusted proportionately based on the used amount of Fe_3O_4 NPs.

Preparation of spinning solutions for fabricating hollow nanofibers

In the preparation of spinning solutions, CSA was dissolved in 2.5000 g of DMF with magnetic stirring at room temperature, then ANI and 1.0000 g of $CHCl_3$ were slowly added into the above solution, and PVP was added into the mixture with stirring as a viscosity improver and template for electrospinning process.

The pre-blended solution was then cooled down to 0 °C in an ice-bath. APS was acted as an oxidant and dispersed into 2.0000 g of DMF at 0 °C and then slowly added into the above solution with magnetic stirring. The final mixture was allowed to react for 24 h at 0 °C and PANI was obtained by the polymerization of aniline[36]. Finally, a certain amount of the as-prepared Fe_3O_4 NPs were ultrasonically dispersed into 2.0000 g of $CHCl_3$ for 20 min and added into the PANI solution. Then $Eu(BA)_3phen$ powders were also dissolved into the above emulsion under magnetic stirring for 12 h at room temperature, thus the spinning solution was obtained. In order to find the optimum ratio of $Eu(BA)_3phen$ and PANI, different spinning solutions containing various amounts of $Eu(BA)_3phen$ and PANI were respectively prepared, followed by introducing various amounts of APS and CSA. Besides, to investigate the impact of Fe_3O_4 NPs on the magnetic and fluorescent properties of the hollow nanofibers, various amounts of Fe_3O_4 NPs were introduced into spinning solutions. The dosages of these materials were listed in Table 1, and the products produced by spinning solutions 1-9 were denoted as S_1-S_9, respectively.

Table 1 Compositions of the spinning solutions

Spinning solutions	Compositions					
	ANI/g	CSA/g	APS/g	$Eu(BA)_3phen$/g	Fe_3O_4/g	PVP/g
1	0.18	0.2245	0.4411	0.7200	0.2000	0.6000
2	0.18	0.2245	0.4411	0.9000	0.2000	0.6000
3	0.18	0.2245	0.4411	1.0800	0.2000	0.6000
4	0.18	0.2245	0.4411	1.2600	0.2000	0.6000
5	0.12	0.1497	0.2940	1.0800	0.2000	0.6000
6	0.24	0.2993	0.5881	1.0800	0.2000	0.6000
7	0.18	0.2245	0.4411	1.0800	0.3000	0.6000
8	0.18	0.2245	0.4411	1.0800	0.6000	0.6000
9	0.18	0.2245	0.4411	1.0800	1.2000	0.6000

Fabrication of $Eu(BA)_3phen$/PANI/Fe_3O_4/PVP flexible hollow nanofibers via one-pot electrospinning

A homemade setup for coaxial electrospinning was used in this study as depicted in Fig. 1a. The as-prepared spinning solution was loaded into the outer plastic syringe, while the inner plastic syringe was empty but the air. The coaxial needle was composed of a truncated 8 # stainless steel needle as the inner one and a truncated 16 # stainless steel needle as the outer one, and the tip of the inner needle protruded 0.5 mm out of the outer needle. A flat iron net was put about 12 cm away from the tip of the coaxial needle as a fiber collector. A positive direct current (DC) voltage of 11 kV was applied between the needle and the collector to generate stable, continuous PVP-based photoluminescent-electrical-magnetic trifunctional flexible hollow nanofibers at the room temperature of 10-15 °C, and the relative humidity was 20-25 %. As seen from the endpoint of the collected nanofibers, hollow structure can be formed via coaxial electrospinning process. The section diagram of the as-prepared hollow nanofibers containing europium complex, PANI and Fe_3O_4 NPs is illustrated in Fig. 1b. The interactions among components are provided in the Electronic Supplementary Information.

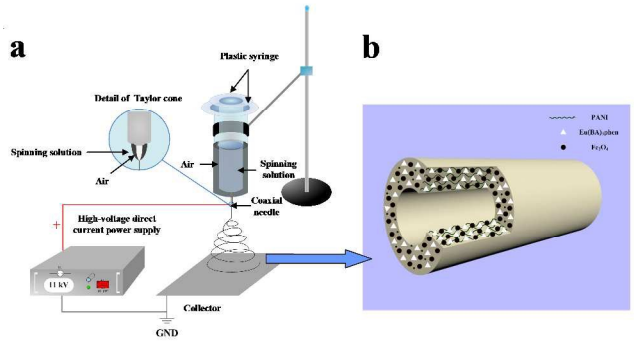

Fig. 1 Schematic illustration of the setup for one-pot coaxial electrospinning process (a) and the as-prepared hollow nanofibers containing europium complex, PANI and Fe_3O_4 NPs (b).

2.3 Characterization methods

The phase compositions of samples were identified by an X-ray powder diffractometer (XRD, Bruker, D8 FOCUS) with Cu Ka radiation. The operation voltage and current were kept at 40 kV and 20 mA, respectively. The morphology and internal structure of the as-prepared hollow nanofibers were observed by a field-emission scanning electron microscope (FESEM, XL-30) and a transmission electron microscope (TEM, JEM-2010), respectively. The elemental analysis was performed by an energy-dispersive spectrometer (EDS, Oxford Instruments) attached to the FESEM. Then, the fluorescent performances of $Eu(BA)_3phen$/PANI/Fe_3O_4/PVP hollow nanofibers were investigated by Hitachi fluorescence spectrophotometer F-7000. The UV-Vis absorption spectra were measured by a UV-Vis spectrophotometer (SHIMADZU UV mini 1240). The electrical conductivities of samples were determined by a 4-point probes resistivity measurement system (RTS-9 type). The magnetic properties were measured by a vibrating sample magnetometer (VSM, MPMS SQUID XL). The Fourier-transform infrared spectra (FT-IR) were tested by a Shimadzu model 8400s FT-IR spectrophotometer with KBr pellet technique. All the measurements were performed at room temperature.

3 Results and discussion

3.1 Phase analyses

In order to investigate the phase compositions of the Fe_3O_4 NPs and $Eu(BA)_3phen$/PANI/Fe_3O_4/PVP hollow nanofibers, XRD was employed to analyze the samples. As shown in Fig. 2, the positions of diffraction peaks match well with the PDF 74-0748 standard card of Fe_3O_4, which indicates that the Fe_3O_4 NPs are single phase and belong to the cubic system. Moreover, no characteristic peaks are observed for other impurities such as Fe_2O_3 and FeO(OH). For hollow nanofibers, it is obvious that the hollow nanofibers contain Fe_3O_4 NPs.

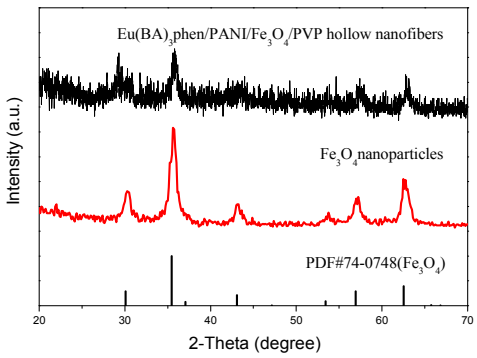

Fig. 2 XRD patterns of Fe_3O_4 NPs and $Eu(BA)_3phen/PANI/Fe_3O_4/PVP$ hollow nanofibers with the PDF standard card of Fe_3O_4.

3.2 Structure and formation mechanism

Morphology and internal structure

The morphology of $Eu(BA)_3phen/PANI/Fe_3O_4/PVP$ hollow nanofibers was characterized by the combination of SEM, TEM, and EDS analyses. As illustrated in Fig. 3, FESEM observation (Fig. 3a) indicates that the electrospun hollow nanofibers orientate randomly and interweave to form a network structure. A magnified FESEM image (Fig. 3a, inset) clearly reveals that the nanofibers possess a typical hollow structure. Moreover, the surface of the flexible hollow nanofibers is relatively smooth and the nanofibers have almost uniform outer diameters of 305 ± 1.7 nm as shown in Fig. 3b and inner diameters of *ca.* 140 nm. Fig. 3c shows the EDS analysis of the as-prepared hollow nanofibers, which confirms the presence of C, N, O, S, Fe, Eu and Au elements in the hollow nanofibers. The Au peak in the spectrum comes from gold conductive film plated on the surface of the sample for SEM observation.

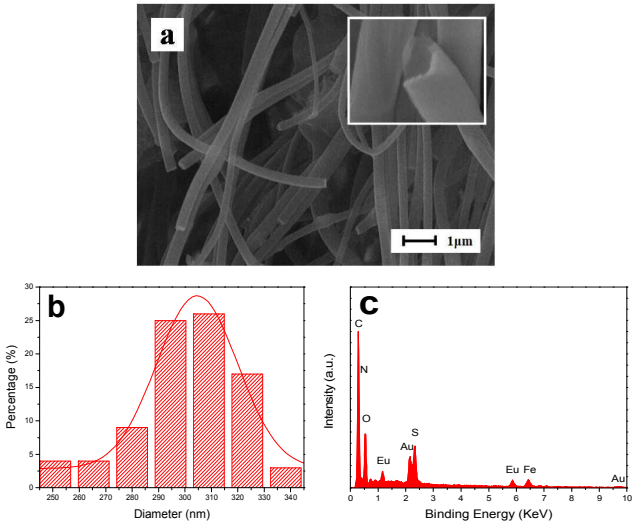

Fig. 3 FESEM image (a), histogram of diameter distribution (b), and EDS spectrum (c) of the $Eu(BA)_3phen/PANI/Fe_3O_4/PVP$ hollow nanofibers.

The internal structure of the nanofibers was further investigated by using TEM technique, as presented in Fig. 4. Clear hollow structures can be observed with inner diameters of *ca.* 140 nm, which is consistent with the result of SEM analysis. The Fe_3O_4 NPs are uniformly dispersed in the shell of the hollow nanofibers. From the above analyses, we can safely conclude that the $Eu(BA)_3phen/PANI/Fe_3O_4/PVP$ hollow nanofibers have been successfully fabricated.

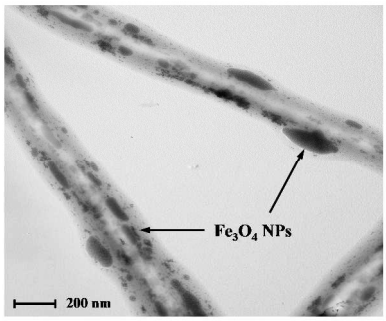

Fig. 4 TEM image of the $Eu(BA)_3phen/PANI/Fe_3O_4/PVP$ hollow nanofibers.

Formation mechanism of the as-prepared hollow nanofibers

As seen from the endpoints of the as-prepared hollow nanofibers in Fig. 3a, the successful fabrication of $Eu(BA)_3phen/PANI/Fe_3O_4/PVP$ hollow nanofibers can be ascribed to the fact that the air flowed down from the inner needle has the ability to support the hollow structure of the Taylor cone and the subsequent electrospun nanofibers. Upon our previous study we find that the $CHCl_3$ used as an necessary part of solvent in the spinning solution plays an important role in the formation of the hollow structure which can be discussed in detail for the following reasons: (a) The electrospinning rate is faster when $CHCl_3$ exists in the spinning solution due to its lower surface tension, and the spinning solution in the Taylor cone can be jetted out in a short time, so that the Taylor cone and the spun nanofibers can retain hollow structures. Conversely, when no $CHCl_3$ is used, the surface tension of the spinning solution is high, leading to a slow spinning rate. Because the support ability of air is not strong enough to retain the hollow structure of the Taylor cone for a long time, the hollow-structured Taylor cone will turn into a solid-structured Taylor cone due to the contraction of the spinning solution; (b) The evaporation rate of $CHCl_3$ is so fast that the morphology of the spun hollow nanofibers can be rapidly fixed and retained in a short period after forming the jet, on the contrary, the hollow core of the fibers may be closed due to the diffusion of the residual solvent if the solvent in the jet evaporates too slowly, as shown in the part Ⅰ of Fig. 5. Besides the impact of the $CHCl_3$ on the formation of the hollow structure, as seen from the part Ⅱ of Fig. 5, another influencing factor is high-voltage. If the voltage is over-high, the spinning solution will be jetted out near the tip edge of the outer needle so that the Taylor cone is not hollow-structured, and the fabricated nanofibers were not hollow-structured as well. Furthermore, an over-high voltage has a negative impact on the formation of the nanofibers, which leads to an uneven diameter distribution of the nanofibers. Therefore, an appropriate voltage should be applied to construct stable photoluminescent-electrical-magnetic trifunctional flexible hollow nanofibers.

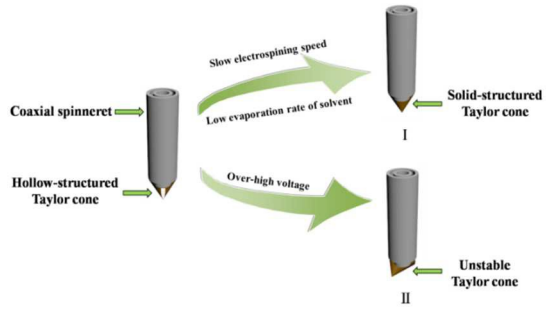

Fig. 5 Schematic diagram of the Taylor cone structure under different cases in the formation of the as-prepared hollow nanofibers.

3.3 Photoluminescent performance

The performance of luminescent materials is influenced by the doping emitter concentration, so it is of great significance to determine the optimum concentration for the as-prepared hollow nanofibers. To perform this study, a series of $Eu(BA)_3phen/PANI/Fe_3O_4/PVP$ hollow nanofibers were fabricated. The mass percentage of PANI to PVP and the mass ratio of Fe_3O_4 to PVP were fixed at 30 % and 1:3, respectively. Fig. 6 demonstrates the excitation and emission spectra of $Eu(BA)_3phen/PANI/Fe_3O_4/PVP$ hollow nanofibers with different doping concentrations of $Eu(BA)_3phen$ from 120 % to 210 % (samples S_1-S_4). When monitored at 616 nm, the excitation spectra (Fig. 6, left) exhibit broad bands extending from 200 to 350 nm with a maximum intensity at 306 nm, which is attributed to the $\pi \rightarrow \pi^*$ electronic transition of the ligands. The emission spectra of the samples are recorded at an excitation wavelength of 306 nm, as shown in the right part of Fig. 6. A series of characteristic emission peaks between 550 nm and 700 nm can be observed due to the energy level transitions of $^5D_0 \rightarrow {}^7F_0$ (580 nm), $^5D_0 \rightarrow {}^7F_1$ (592 nm) and $^5D_0 \rightarrow {}^7F_2$ (616 nm) of Eu^{3+} ions, and the predominant emission peaks at 616 nm correspond to the $^5D_0 \rightarrow {}^7F_2$ hypersensitive transition. Furthermore, when the mass percentages of $Eu(BA)_3phen$ are varied from 120 % to 180 %, both the excitation and emission intensity markedly increase, and then only slightly increase when the mass percentages of $Eu(BA)_3phen$ continue to increase from 180 % to 210 %, as more clearly seen from the inset of Fig. 6. Therefore, the mass percentage of $Eu(BA)_3phen$ of 180 % was adopted to prepare the $Eu(BA)_3phen/PANI/Fe_3O_4/PVP$ hollow nanofibers.

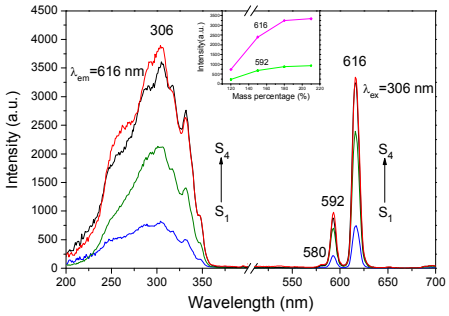

Fig. 6 Excitation (left) and emission spectra (right) of $Eu(BA)_3phen/PANI/Fe_3O_4/PVP$ hollow nanofibers containing different mass percentages of $Eu(BA)_3phen$: 120 % (S_1), 150 % (S_2), 180 % (S_3), 210 % (S_4); Inset: relationships between $Eu(BA)_3phen$ contents and intensity of luminescent peaks at 616 nm and 592 nm for $Eu(BA)_3phen/PANI/Fe_3O_4/PVP$ hollow nanofibers.

Additionally, a comparative study is carried out to demonstrate the effect of adding different amounts of PANI and Fe_3O_4 NPs on the photoluminescence properties of the hollow nanofibers. Firstly, the influence of PANI on the photoluminescence property is researched. The mass percentage of $Eu(BA)_3phen$ to PVP and the mass ratio of Fe_3O_4 NPs to PVP were fixed at 180 % and 1:3, respectively. $Eu(BA)_3phen/PANI/Fe_3O_4/PVP$ hollow nanofibers containing different mass percentages of PANI ranging from 20 % to 40 % were fabricated (samples S_3, S_5-S_6). It can be seen from Fig. 7a that the photoluminescence intensities decrease with the increasing amounts of PANI, which results from the light absorption of PANI mixed in the hollow nanofibers. Especially when the mass percentage of PANI is 40 %, the photoluminescence peaks decrease significantly. The UV-Vis absorbance spectrum of PANI/PVP nanofibers shown in Fig. 7b clearly explains that PANI/PVP can strongly absorb ultraviolet light (300-400 nm) and visible light (400-900 nm).

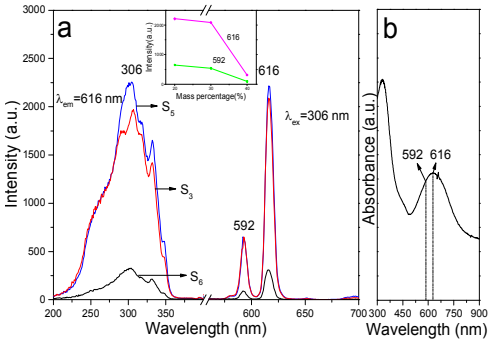

Fig. 7 Comparison of photoluminescence spectra of $Eu(BA)_3phen/PANI/Fe_3O_4/PVP$ hollow nanofibers containing different mass percentages of PANI (a) and UV-Vis absorbance spectrum of PANI/PVP nanofibers (b).

As illustrated in Fig. 8, the exciting light and emitting light in the hollow nanofibers are absorbed by PANI, resulting in that the intensities of exciting light and emitting light are decreased, and the light absorption becomes stronger with introducing more PANI into the hollow nanofibers. Generally, fluorescence color can be represented by the Commission Internationale de L'Eclairage (CIE) 1931 chromaticity coordinates. Fig. 9 depicts the CIE coordinate diagram of $Eu(BA)_3phen/PANI/Fe_3O_4/PVP$ hollow nanofibers with different percentages of PANI under the excitation of 306-nm ultraviolet light. It demonstrates that the emitting color of $Eu(BA)_3phen/PANI/Fe_3O_4/PVP$ hollow nanofibers becomes lighter with introducing more PANI, due to the stronger absorption of red light by PANI.

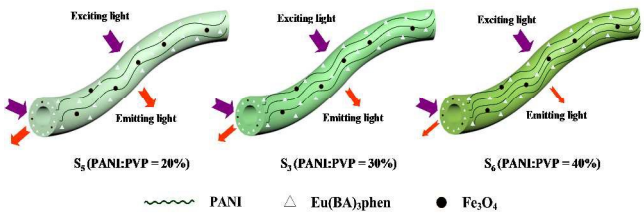

Fig. 8 Schematic diagram of the situation of the exciting light and emitting light in $Eu(BA)_3phen/PANI/Fe_3O_4/PVP$ hollow nanofibers containing different percentages of PANI.

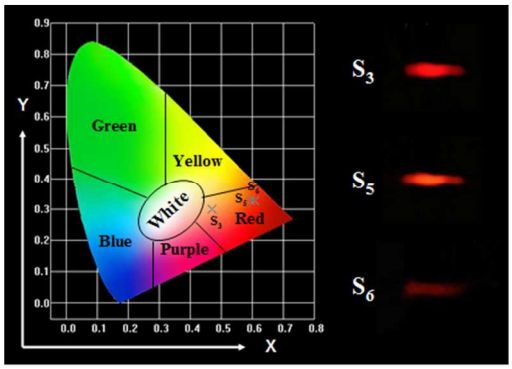

Fig. 9 CIE chromaticity coordinates diagram of $Eu(BA)_3phen/PANI/Fe_3O_4/PVP$ hollow nanofibers containing different percentages of PANI.

Subsequently, the influence of Fe_3O_4 NPs on the photoluminescence property is also studied. The mass percentage of $Eu(BA)_3phen$ to PVP and that of PANI to PVP were maintained at 180 % and 30 %, respectively. $Eu(BA)_3phen/PANI/Fe_3O_4/PVP$ hollow nanofibers containing different mass ratios of Fe_3O_4 NPs were fabricated (samples S_3, S_7-S_9). It is observed by comparing the photoluminescence spectra in Fig. 10a that the photoluminescence intensities decrease with the increasing amounts of Fe_3O_4 NPs introduced into the hollow nanofibers. This phenomenon can be explained by the absorbance spectrum of Fe_3O_4 NPs illustrated in Fig. 10b, which shows that light absorption of the dark-colored Fe_3O_4 NPs at ultraviolet wavelengths ($\lambda < 400$ nm) is much stronger than that in visible region ($\lambda = 400$-760 nm).

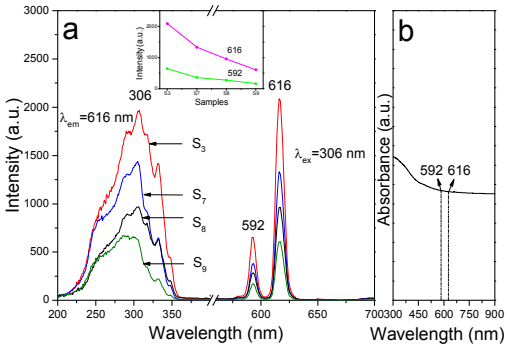

Fig. 10 Comparison of photoluminescence spectra of $Eu(BA)_3phen/PANI/Fe_3O_4/PVP$ hollow nanofibers containing different mass ratios of Fe_3O_4 NPs (a) and UV-Vis absorbance spectrum of Fe_3O_4 NPs (b).

As revealed in Fig. 11, the exciting light and emitting light in the hollow nanofibers are absorbed by Fe_3O_4 NPs, leading to the fact that the intensities of exciting light and emitting light are decreased, and the light absorption becomes stronger with introducing more Fe_3O_4 NPs into the hollow nanofibers. Fig. 12 is the CIE coordinate diagram of $Eu(BA)_3phen/PANI/Fe_3O_4/PVP$ hollow nanofibers with different mass ratios of Fe_3O_4 NPs under the excitation of 306-nm ultraviolet light. It demonstrates that the emitting color of $Eu(BA)_3phen/PANI/Fe_3O_4/PVP$ hollow nanofibers becomes darker with introducing more Fe_3O_4 NPs, which can be attributed to the fact that Fe_3O_4 NPs have stronger light absorption at ultraviolet range.

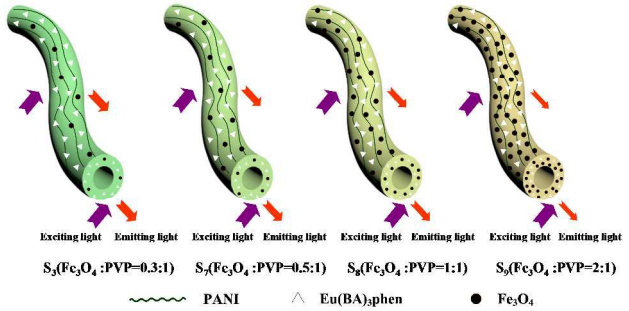

Fig. 11 Schematic diagram of the situation of the exciting light and emitting light in $Eu(BA)_3phen/PANI/Fe_3O_4/PVP$ hollow nanofibers containing different mass ratios of Fe_3O_4 NPs.

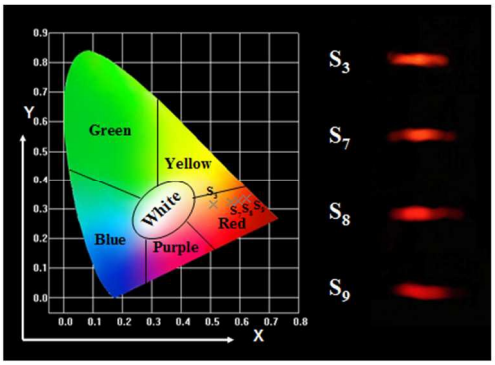

Fig. 12 CIE chromaticity coordinates diagram of $Eu(BA)_3phen/PANI/Fe_3O_4/PVP$ hollow nanofibers containing different mass ratios of Fe_3O_4 NPs.

Thus, it is concluded that the existence of PANI and Fe_3O_4 NPs leads to the decrease in photoluminescence intensities, and furthermore, photoluminescence intensities become much weaker with more PANI and Fe_3O_4 NPs introduced into the hollow nanofibers.

3.4 Electrical conductivity analyses

Except for the above photoluminescence property, the electrical conductivity of the trifunctional flexible hollow nanofibers is also researched. PANI is known as a conducting polymer and is distributed consecutively in the $Eu(BA)_3phen/PANI/Fe_3O_4/PVP$ hollow nanofibers. Hence the introduction of more PANI into the hollow nanofibers facilitates the formation of continuous conductive network with more efficient charge transport, leading to enhancement in electrical conductivity of the hollow nanofibers. As summarized in Table 2, the average electrical conductivity values of the hollow nanofibers increase greatly from 2.70×10^{-4} to 3.46×10^{-3} $S\cdot cm^{-1}$ when the mass percentages of PANI are varied from 20 % to 30 %. With further increase in amount of PANI, the conductivity of the hollow nanofibers changes slightly. Combined with the above results of photoluminescence spectra analyses, it is evidenced that the optimum mass percentage of PANI to PVP is 30 %. Besides, when fixing other parameters, the samples doped with various amounts of Fe_3O_4 NPs (S_7-S_9) are tested to discuss the effect of Fe_3O_4 NPs on the electrical conductivity, and the results demonstrate that the presence of Fe_3O_4 NPs has little influence on the conductivities of the samples.

Table 2 Electrical conductivity of the samples doped with various amounts of PANI and Fe_3O_4 NPs

Samples	Various amounts	Electrical conductivity ($S \cdot cm^{-1}$)
S_5	PANI:PVP=20 %	2.70×10^{-4}
S_3	PANI:PVP=30 %	3.46×10^{-3}
S_6	PANI:PVP=40 %	4.03×10^{-3}
S_7	Fe_3O_4:PVP=0.5:1	2.96×10^{-3}
S_8	Fe_3O_4:PVP=1:1	3.48×10^{-3}
S_9	Fe_3O_4:PVP=2:1	3.75×10^{-3}

3.5 Magnetic properties

Hysteresis loops of Fe_3O_4@OA NPs and Eu(BA)$_3$phen/PANI/Fe_3O_4/PVP hollow nanofibers containing different mass ratios of Fe_3O_4 NPs are used to confirm the magnetic properties of the samples, as shown in Fig. 13, and their saturation magnetizations are listed in Table 3. Magnetic measurements illustrate that the saturation magnetization value of the as-prepared Fe_3O_4@OA NPs is 40.34 $emu \cdot g^{-1}$ and neither remanence nor coercivity is detected. And the reversible hysteresis behavior also indicates the Fe_3O_4 NPs exhibit superparamagnetism and fast magnetic responsivity. It should be noted that the trifunctional flexible hollow nanofibers still show good paramagnetism. From Table 3, it is clear that the saturation magnetizations of the hollow nanofibers increase from 3.09 $emu \cdot g^{-1}$ to 12.59 $emu \cdot g^{-1}$ with the increasing amount of Fe_3O_4 NPs. Hence, the magnetic properties of the hollow nanofibers can be tuned by adding various contents of Fe_3O_4 NPs.

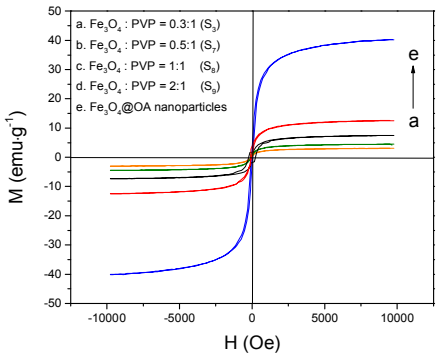

Fig. 13 Hysteresis loops of Fe_3O_4@OA NPs and Eu(BA)$_3$phen/PANI/Fe_3O_4/PVP hollow nanofibers containing different mass ratios of Fe_3O_4 NPs.

Table 3 Saturation magnetization of Fe_3O_4@OA NPs and Eu(BA)$_3$phen/PANI/Fe_3O_4/PVP hollow nanofibers containing different mass ratios of Fe_3O_4 NPs

Samples	Saturation magnetization (M)/$emu \cdot g^{-1}$
Fe_3O_4@OA NPs	40.34
Fe_3O_4 : PVP = 2:1 (S_9)	12.59
Fe_3O_4 : PVP = 1:1 (S_8)	7.51
Fe_3O_4 : PVP = 0.5:1 (S_7)	4.51
Fe_3O_4 : PVP = 0.3:1 (S_3)	3.09

4 Conclusions

In summary, we have developed a novel strategy for directly fabricating photoluminescent-electrical-magnetic trifunctional flexible Eu(BA)$_3$phen/PANI/Fe_3O_4/PVP hollow nanofibers via one-pot electrospinning. The mean diameter and the inner diameter of the hollow nanofibers are *ca.* 305 nm and *ca.* 140 nm, respectively. It is very gratifying to see that the hollow nanofibers possess excellent photoluminescent performance, electrical conductivity and magnetic properties. Furthermore, the photoluminescent intensity, electrical conductivity and magnetic properties of the hollow nanofibers can be tuned by adding different concentration of the luminescent material, as well the contents of PANI and Fe_3O_4 NPs, respectively. Based on this design conception and synthetic strategy, other photoluminescent-electrical-magnetic trifunctional hollow nanofibers can be fabricated. For instance, the photoluminescent color of the hollow nanofibers is tunable by adjusting the diversity and contents of the luminescent materials. Owing to these versatile properties, the novel hollow fibrous structured trifunctional material is expected to apply in various areas of electromagnetic interference shielding, molecular electronics, multifunctional nanodevices and biomedical field, etc.

Acknowledgements

This work was financially supported by the National Natural Science Foundation of China (NSFC 50972020, 51072026), Specialized Research Fund for the Doctoral Program of Higher Education (20102216110002, 20112216120003), the Science and Technology Development Planning Project of Jilin Province (Grant Nos. 20130101001JC, 20070402).

Notes and references

Key Laboratory of Applied Chemistry and Nanotechnology at Universities of Jilin Province, Changchun University of Science and Technology, Changchun 130022. Fax: 86 0431 85383815; Tel: 86 0431 85582574; E-mail: dongxiangting888@163.com

1. Y. Sun, L. Zhang, Y. Wang, P. Chen, S. Xin, H. Jiu and J. Liu, *J. Alloys Compd.*, 2014, **586**, 441.
2. G. Yang, R. Lv, S. Gai, Y. Dai, F. He and P. Yang, *Inorg. Chem.*, 2014, **53**, 10917.
3. J. P. Cheng, B. B. Wang, M. G. Zhao, F. Liu and X. B. Zhang, *Sens. Actuators, B*, 2014, **190**, 78.
4. S. Peng, L. Li, Y. Hu, M. Srinivasan, F. Cheng, J. Chen and S. Ramakrishna, *ACS Nano*, 2015, **9**, 1945.
5. C. Y. Tay, M. I. Setyawati, J. Xie, W. J. Parak and D. T. Leong, *Adv. Funct. Mater.*, 2014, **24**, 5936.
6. L. Cheng, S. Y. Ma, T. T. Wang, X. B. Li, J. Luo, W. Q. Li, Y. Z. Mao and D. J. Gz, *Mater. Lett.*, 2014, **131**, 23.
7. J. Jung, D. Lee and Y. Lee, *J. Alloys Compd.*, 2015, **622**, 651.
8. D. Hou, X. Hu, W. Ho, P. Hu and Y. Huang, *J. Mater. Chem. A*, 2015, **3**, 3935.
9. C. Mi, J. Zhang, H. Gao, X. Wu, M. Wang, Y. Wu, Y. Di, Z. Xu, C. Mao and S. Xu, *Nanoscale*, 2010, **2**, 1141.
10. S. Yu, X. Gao, H. Jing, R. Zhang, X. Gao and H. Su, *CrystEngComm*, 2014, **16**, 6645.

11. S. Som, P. Mitra, V. Kumar, V. Kumar, J. J. Terblans, H. C. Swart and S. K. Sharma, *Dalton Trans.*, 2014, **43**, 9860.
12. Z. Y. Ma, D. Dosev, M. Nichkova, S. J. Gee, B. D. Hammock and I. M. Kennedy, *J. Mater. Chem.*, 2009, **19**, 4695.
13. Y. Liu, Z. Wang, G. Cheng, J. Zhang, G. Hong and J. Ni, *Mater. Lett.*, 2015, **152**, 224.
14. S. Gai, P. Yang, C. Li, W. Wang, Y. Dai, N. Niu and J. Lin, *Adv. Funct. Mater.*, 2010, **20**, 1166.
15. Q. Ma, J. Wang, X. Dong, W. Yu and G. Liu, *Chem. Eng. J.*, 2013, **222**, 16.
16. Q. Ma, J. Wang, X. Dong, W. Yu and G. Liu, *ChemPlusChem*, 2014, **79**, 290.
17. H. Wang, Y. Li, L. Sun, Y. Li, W. Wang, S. Wang, S. Xu and Q. Yang, *J. Colloid Interface Sci.*, 2010, **350**, 396.
18. F. Huang, H. Zhang, J. Shi, F. Chen, Y. Cai and Q. Wei, *Int. J. Mater. Res.*, 2012, **103**, 1390.
19. N. Lv, X. Dong, Q. Ma, J. Wang, W. Yu and G. Liu, *J Mater Sci*, 2014, **49**, 2171.
20. X. Lu, C. Wang and Y. Wei, *Small*, 2009, **5**, 2349.
21. L. Huang, J. T. Arena, S. S. Manickam, X. Jiang, B. G. Willis and J. R. McCutcheon, *J. Membr. Sci.*, 2014, **460**, 241.
22. Z. Hou, G. Li, H. Lian and J. Lin, *J. Mater. Chem.*, 2012, **22**, 5254.
23. C. Peng, M. Shang, G. Li, Z. Hou, D. Geng and J. Lin, *Dalton Trans.*, 2012, **41**, 4780.
24. S. N. Jayasinghe, *Analyst*, 2013, **138**, 2215.
25. Y. Mizuno, E. Hosono, T. Saito, M. Okubo, D. Nishio-Hamane, K. Oh-ishi, T. Kudo and H. Zhou, *J. Phys. Chem. C*, 2012, **116**, 10774.
26. J. Song, M. Chen, M. B. Olesen, C. Wang, R. Havelund, Q. Li, E. Xie, R. Yang, P. Boggild, C. Wang, F. Besenbacher and M. Dong, *Nanoscale*, 2011, **3**, 4966.
27. X. Chen, F. Zhang, Q. Wang, X. Han, X. Li, J. Liu, H. Lin and F. Qu, *Dalton Trans.*, 2015, **44**, 3034.
28. A. L. Yarin, *Polym. Adv. Technol.*, 2011, **22**, 310.
29. J. T. McCann, D. Li and Y. Xia, *J. Mater. Chem.*, 2005, **15**, 735.
30. X. Ji, P. Wang, Z. Su, G. Ma and S. Zhang, *J. Mater. Chem. B*, 2014, **2**, 181.
31. Q. Ma, J. Wang, X. Dong, W. Yu and G. Liu, *Adv. Funct. Mater.*, 2015, **25**, 2436.
32. G. Lee, J. Song and K. Yoon, *Macromol. Res.*, 2010, **18**, 571.
33. D. Li, J. Wang, X. Dong, W. Yu and G. Liu, *J Mater Sci*, 2013, **48**, 5930.
34. S. Meshkova, *J. Fluoresc.*, 2000, **10**, 333.
35. Y. Y. Zheng, X. B. Wang, L. Shang, C. R. Li, C. Cui, W. J. Dong, W. H. Tang and B. Y. Chen, *Mater. Charact.*, 2010, **61**, 489.
36. N. Gospodinova and L. Terlemezyan, *Prog. Polym. Sci.*, 1998, **23**, 1443.